Numerical research on whispering-gallery modes in a triple-layer-coated microsphere resonator *

WANG Meng-yu (王梦宇)**, JIN Xue-ying** (金雪莹)**, and WANG Ke-yi** (王克逸)**
Department of Precision Machinery and Precision Instrumentation, University of Science and Technology of China, Hefei 230027, China

(Received 14 April 2018; Revised 24 May 2018)

We numerically demonstrate that whispering-gallery modes (WGMs) in a microsphere resonator with three layers of high, low and high refractive index (RI) are analyzed by using the finite difference time domain (FDTD) method. To make the light couple in and out of the microsphere, a phase matched waveguide is used to overlap the WGMs evanescent radiation field. By changing the gap between the microsphere and waveguide, the WGMs of two high-RI layers are efficiently excited. The stored energy and the mode volume are optimized for sensing applications. The coupling structure reveals a good sensitivity of 38.29 nm/RIU (RI unit).
Document code: A **Article ID:** 1673-1905(2018)05-0331-5
DOI https://doi.org/10.1007/s11801-018-8056-3

Optical resonators on the microscale and nanoscale play an extremely important role in modern optics, not only as a fundamental device for lasers, but also as etalons for optical filters and tools for very accurate measurements[1]. In recent years, dielectric resonators supported whispering-gallery modes (WGMs) have attracted increasing attention, a growing number of papers have been published, investigating structures from the simplest ones, namely microspheres, microdisks, microtoroids, up to the most exotic structures, such as bottle and bubble microresonators[2]. These WGM microresonators can have an extremely high quality (Q) factor that makes them promising devices for applications in optoelectronics and experimental physics[3-5]. In generally, the WGMs in microsphere strongly confined just the inside surface by continuous total internal reflection (TIR), leading to Q factors in excess of 10^8[3]. Due to the advantages of high Q factors and low mode volumes, microspheres are widely used as optical refractive-index (RI) sensors for a variety of applications, such as measuring chemical composition, probing concentration changes and detecting biological materials[6], For example, a fused silica microsphere sensor was proposed to detect protein molecule, virus particles and RI change of the surrounding medium[7,8].

Coating of the resonator is a very prospective technique for optimizing optical properties of the microspheres. In the recent year, most of the work in sensing field has focused on the characteristics of coating in the microspheres[9,10]. Teraoka and Arnold et al[9] have calculated WGMs in a dielectric microsphere coated with a high-RI layer. They proposed that a RI coating with appropriate thickness can compress the electromagnetic (EM) field distribution in the radial direction and enhance the sensitivity in high-sensitivity sensor application. Additionally, the finite difference time domain (FDTD) method is the most commonly acknowledged numerical model to analyze the micro-resonator structure[11]. It is extremely effective to analyze the optimal design associated with these kinds of WGM micro-resonators and predict the EM field and energy distributions precisely.

Previously, the dispersion characteristics of a microsphere via multi-layer coating were present using a modified Mie scattering theory[12]. In this paper, we report the numerical research of the WGMs in a triple-layer-coated microsphere resonator. The WGMs in a microsphere wrapped up with three layers of high, low and high RI are numerically analyzed by using FDTD method. We demonstrate by calculations that the effect of three-layer coatings by changing the gap distance between the microsphere and waveguide. The stored energy and the mode volume can be optimized by tailoring the thickness of the low-RI layer for sensing application.

The three mode number (l, m, n), where l, m and n are the EM field components along radial, angular and azimuthal directions, identifies the modes of WGMs[13]. The resonance inside the microsphere presents typically a brilliant equatorial ring on the equator plane. It is suitable to utilize a two-dimensional (2D) numerical model to describe the course to excite the WGMs in this study. Let us consider a homogeneous microsphere structure

* This work has been supported by the National Natural Science Foundation of China (Nos.61775209 and 61275011).
** E-mail: kywang@mail.ustc.edu.cn

coated by three layers with high, low and high RI from inside to outside as depicted in Fig.1(a). The intrinsic microsphere can be produced by melting the tip of standard optical telecommunications fibers[14]. Furthermore, the film thickness needs to be accurately controlled, which can be fabricated by a magnetron sputtering coating machine. The radio frequency (RF) sputtering method exactly controls the thickness of the coating film in silica microresonators[15,16]. We design a 2D FDTD numerical model to study this structure as shown in Fig.1(b). The thicknesses of three layers (A, B, C) are d_A, d_B and d_C, and the RIs of three layers are n_A, n_B and n_C, respectively. The total radius of the microsphere is R. The electric field on the radial distribution $S(r)$ for transverse electric (TE) polarization mode can be given as

$$S(r)=\begin{cases} A\psi_l(n_1kr) & r<R-d_A-d_B-d_C \\ C_l\psi_l(n_Ckr)+D_l\chi_l(n_Ckr) & R-d_A-d_B-d_C<r<R-d_A-d_B \\ C_{l2}\psi_l(n_Bkr)+D_{l2}\chi_l(n_Bkr) & R-d_A-d_B<r<R-d_A \\ C_{l3}\psi_l(n_Akr)+D_{l3}\chi_l(n_Akr) & R-d_A<r<R \\ B\psi_l(n_0kr) & r>R \end{cases}, \quad (1)$$

where $\psi_l(z)\equiv zJ_l(z)$ and $\chi_l(z)\equiv zn_l(z)$ are the spherical Ricatti-Bessel and the Ricatti-Neumann functions, where $j_l(z)$ and $n_l(z)$ stand for the spherical Bessel and Neumann functions of the first kind. n_1 and n_0 stand for the RIs of the microsphere and the surrounding medium. These coefficients A_l, B_l, C_{l1}, D_{l1}, C_{l2}, D_{l2}, C_{l3}, D_{l3} are determined by the boundary conditions at $r=R$, $r=R-d_A$, $r=R-d_A-d_B$ and $r=R-d_A-d_B-d_C$.

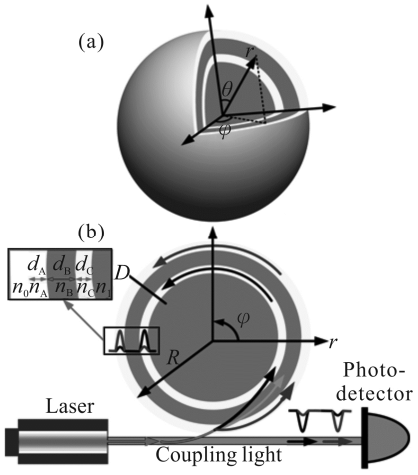

Fig.1 Schematic diagrams of (a) the triple-layer-coated silica microsphere model and (b) the 2D FDTD simulation model coupled by a fiber waveguide

The boundary conditions require the $S(r)$ and $S(r)'$ be continuous across these interfaces. Moreover, $k=2\pi/\lambda_R$ is the resonant wave factor, and λ_R is the resonant wavelength. The characteristic equation to specify λ_R in the resonance spectrum is expressed as

$$\frac{n_B}{n_A}\times\frac{C_{l2}/D_{l2}\times\psi_l'(z_{B2})+\chi_l'(z_{B2})}{C_{l2}/D_{l2}\times\psi_l(z_{B2})+\chi_l(z_{B2})}=\frac{C_{l3}/D_{l3}\times\psi_l'(z_{A1})+\chi_l'(z_{A1})}{C_{l3}/D_{l3}\times\psi_l(z_{A1})+\chi_l(z_{A1})}, \quad (2)$$

where z_{A1} and z_{B2} are given by $z_{A1}=n_Ak(R-d_A)$ and $z_{B2}=n_Bk(R-d_A)$. The electrical field $X(r)$ on the equator plane can be given as

$$X(r)=N_sH_m(m^{1/2}q)\times\exp(-mq^2/2)\times S(r). \quad (3)$$

The simulation domain normally adopts a 13 μm×13 μm rectangular area which is meshed 600×600 grids to ensure the high computational accuracy. A well-known perfectly matched layer (PML) is chosen by absorbing boundary condition (ABC) to meet the calculated grid space in the condition of low reflection. The excitation of the WGMs can be achieved by various approaches, such as tapered fiber, waveguide and prism. Among these approaches, the coupling efficiency can reach the highest value (almost 100%) with the tapered fiber waveguide. Hence, in our numerical model, a fiber waveguide is added to overlap the WGMs evanescent field. A triple-layer-coated microsphere resonator is set in the central position, and a wideband pump laser light beam is placed in the leftmost position of the waveguide and then couples to the microsphere. The gap distance between the waveguide and resonator is g. The materials and RIs of the microsphere and three coating layers are listed in Tab.1. Three layers can confine more light. The surrounding medium is set to be in air with $n_0=1$, and it also can be changed to other surrounding media.

Tab.1 Parameters of the triple-layer-coated microsphere

Parameter	Microsphere	Inner layer (C)	Middle layer (B)	Outer layer (A)
Material	Silica	TiO_2	Silica	TiO_2
RI	1.452	2.38	1.452	2.38

To study the WGMs of such a structure, we firstly calculate the eigen-mode of triple-layer-coated microsphere.The electric field distributions can be shown as Fig.2. We set a fixed radius as R=3.5 μm. To contain the first radial WGMs (l=1) better, the thickness of the low-RI layer (B) is set as d_B=400 nm and the thickness of the two high-RI layers (A, C) are set as $d_A=d_C$=100—300 nm. When the overall thickness of three coated layers ($d_A+d_B+d_C$=800 nm) and the thickness of the low-RI layer (d_B=400 nm) remain unchanged, as a result, three cases (d_A=100 nm, 200 nm and 300 nm) can be calculated.

Two different radial modes are found on A and C, and we call them 'inner mode' (IM) and 'outer mode' (OM). For d_A=100 nm (d_C=300 nm), the electric field energy for the IM is dispersive, which means that the peak range of the first radial WGMs is wide. The result will lead to the reducing of energy density. Meanwhile, the electric field energy for the OM doesn't remain the center of the outer layer. More overflowing energy will result in a low Q factor. Similarly, for d_A=300 nm (d_C=100 nm), the energy density and Q factor are lower than the case for d_A=200 nm (d_C=200 nm). We conclude that IM and OM have a near linear dependence on the thickness of these two high-RI layers, especially when d_A=d_C=200 nm. For this study, electric field distributions for them along the radial direction can be shown in Fig.2(b), which is defined l=1, as discussed in Ref.[10].

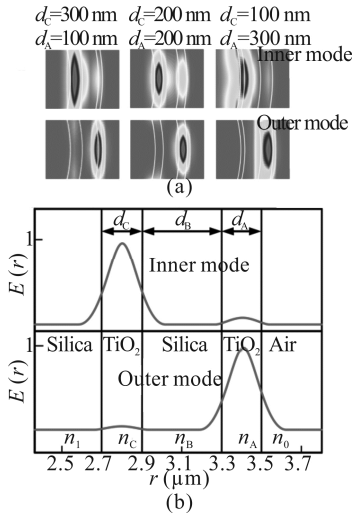

Fig.2 (a) Electric field distributions of the triple-layer-coated microsphere for different coating layers; (b) Inner mode and outer mode along the radial direction with the thickness of three layers with d_A=200 nm, d_B=400 nm, d_C=200 nm

Optical microsphere resonators supporting WGMs used as RI sensors detects RI changes of the surrounding medium through the evanescent field traveling outside the microsphere resonator boundary. The perturbation theory is used to calculate the resonance shift caused by the RI change. RI sensitivity (RIS) $S=\delta\lambda_R/\lambda_R$ is a critical factor for evaluating the device performance. Due to the very small surrounding RI change, the equation can also be applied to our model. When considering an uniform RI change of the surrounding medium δn_0, it can be expressed as

$$S=\frac{\delta\lambda_R}{\lambda_R}=\frac{\int_0^{\infty}\delta(n_0^2)S^2(r)\mathrm{d}r}{2\int_0^{\infty}n^2(r)S^2(r)\mathrm{d}r}\times$$

$$\frac{\delta n_0}{n_0}\times\frac{\int_0^{\infty}\delta(n_0^2)S^2(r)\mathrm{d}r}{2\int_0^{\infty}n^2(r)S^2(r)\mathrm{d}r}=\frac{\delta n_0}{n_0}\times\eta_0, \tag{4}$$

where $n(r)$ is the RI distribution of the coated microsphere on the radial direction, and η_0 denotes the percentage of light energy in the surrounding medium, which can be calculated by FDTD method. Consequently, the RI sensitivity of the IM and OM can be respectively given by

$$S_{n,\mathrm{i}}=\frac{\delta\lambda_{n,\mathrm{i}}}{n_0}\times\eta_{0,\mathrm{i}}\ ,\qquad S_{n,\mathrm{o}}=\frac{\delta\lambda_{n,\mathrm{o}}}{n_0}\times\eta_{0,\mathrm{o}}\ . \tag{5}$$

It should be noted that, in this paper, the subscripts 'i' and 'o' refer to the IM and OM, respectively. It can be seen that the RI sensitivity is proportional to the energy fraction on the surrounding medium.

Secondly, resonant properties are observed by analyzing the relative intensity spectra. The relative intensity spectra of the three-layer coatings as shown in Fig.3 can be got by processing the sample point data (D) after fast Fourier transformation (FFT). The resonance intensity of three-layer is only excited in the inner layer and the outer layer, and resonant wavelengths separate just as the coupling in two different micro-resonators. The OM and IM in two high-RI layers can be excited by waveguide coupling. We set the width of the fiber waveguide to be 300 nm. It is thick enough to support the TE mode, leading to the complete confinement effect of the WGMs inside the coatings. The coupling strength depends on the phase matching between the WGMs in the microsphere and the propagating mode of the waveguide. To excite the WGMs efficiently, the phase matching condition can be optimized by changing the gap (g). As the gap increases, we obtain the resonance relative intensity spectra in three cases, as shown in Fig.3. By changing g, the resonance intensity in these two high-RI layers at λ_R changes constantly. The coupling between the radiation field in the waveguide and the mode in the IM and OM can be optimized by changing the gap. For g=100 nm, the resonance intensity for the IM is too weak, and several OM modes cannot be excited. Beside, for g=200 nm, the resonance intensity for the OM and IM are also weak. Fortunately, the WGMs for the OM and IM can all be efficiently excited in the case of g=150 nm. The high coupling strength means that extremely efficient and controlled power transfer from a fiber waveguide to the microsphere coated three layers is possible.

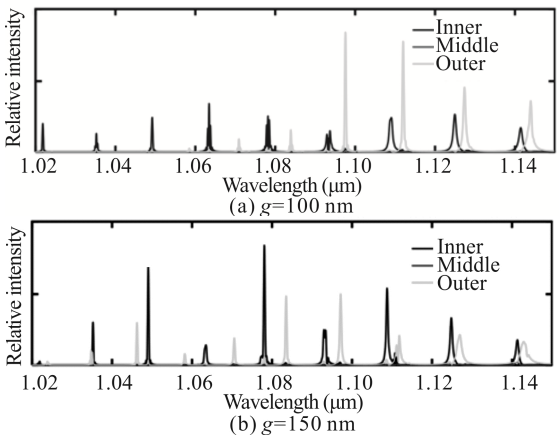

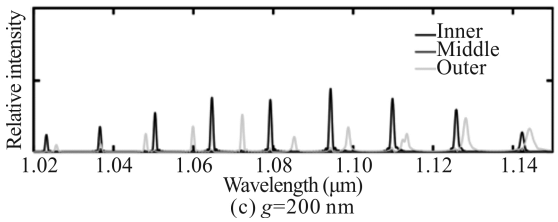

Fig.3 Resonance intensity spectra for different gaps between the microsphere and waveguide with (a) *g*=100 nm, (b) *g*=150 nm and (c) *g*=200 nm

On one hand, to match phase, we calculate the best parameters of d_w=300 nm and g=150 nm. As a result of phase matching, the WGMs of high-RI layers can be efficiently excited. On the other hand, the distance between two high-RI layers, also the thickness of low-RI layer d_B, can be optimized to obtain two strong resonance modes in two high-RI layers. To further optimize the triple-layer resonance structure and study the impact of the coating thickness, we calculate the stored energy ($E_n=\int \varepsilon X^2(r)\mathrm{d}r$) and the mode volume ($V=E_n/\varepsilon X^2(r)_{\max}$) by changing d_B when the resonant intensity of λ_R reaches the maximum value, where ε is the permittivity, as shown in Fig.4. E_n and V are used to describe energy intensity, energy density and give information about field localization. They have a nearly universal influence on micro-resonator across a wide range of applications, especially sensing application. It is obvious that E_n and V become first increase and then decrease in total when d_B varies from 25 nm to 400 nm. We conclude that the highest stored energy ($E_n=11.3\times10^4$) can be obtained when d_B=300 nm. Due to the coupling between two high-RI layers, for small d_B, the resonance peak will be compressed, leading to a larger $X(r)_{\max}$ and a smaller V. For d_B>300 nm, the mode bonding in two high-RI layers is broken, E_n will decrease with the increase of d_B. After optimizing the three-layer structure (d_A=200 nm, d_C=200 nm, d_B=300 nm), its stored energy is almost 1.6 times higher than that of single high-RI layer structure with the coated layer of d=200 nm.

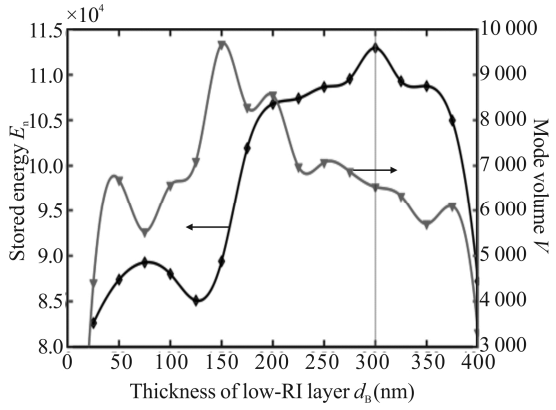

Fig.4 The stored energy and mode volume as a function of the thicknesses of low-RI layer (d_B)

An effortlessly recognizable resonance intensity spectrum is indispensable in many sensing fields. After optimizing the coated structure, we investigate the influence of the surrounding medium on the coupling characteristics and explore the RI sensing application at last. Due to the coupling between IM and OM, the resonant wavelength shift for them all can be selected to detect the RI change of the surrounding medium. Diverse cases under the inner layer and the outer layer resonance are compared as shown as Fig.5. The resonant wavelength for the OM and IM are chosen at 1 074.57 nm and 1 068.43 nm, where the resonant maximum intensity presents. This leads to the very beautiful magnetic field distributions for OM and IM, corresponding to the angular modes of m=36 and m=28. The mode wavelengths are degenerated in respect to the n number, so these two numbers which will determine the mode wavelengths are l and m numbers. The field distributions along the radial direction need be obtained to determine the value of q number. A very brilliant ring with strong electric field can also be found only in the inner layer and the outer layer. The majority of energy stores in these two high-RI layers rather than the middle low-RI layer and the waveguide. In fact, the phase matched conditions give rise to the augment of the light intensity in the region of resonance. The light is favorably constrained inside these two high-RI layers, and TIR occurs.

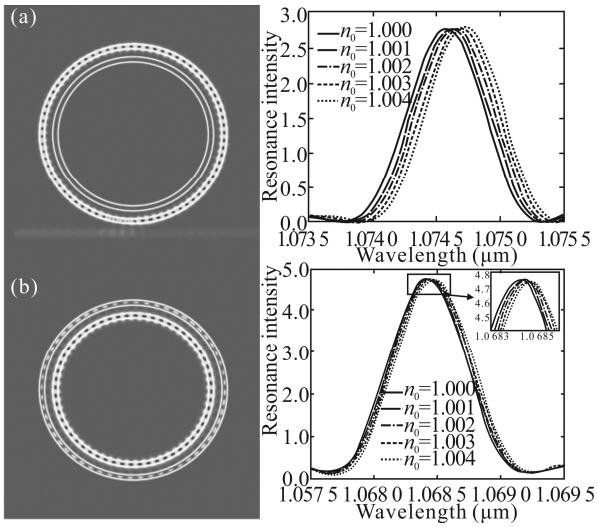

Fig.5 Magnetic field distributions of (a) OM (*m*=36) and (b) IM (*m*=28) and their resonance intensity spectra with RI change of the surrounding medium

To evaluate the sensitivity across these parameters space, the resonance intensity spectra are simulated with the RI of the surrounding medium increasing with increment of 0.001. Other simulation parameters are the same as the optimized parameters. $\delta\lambda_R$ changes as a function of n_0. The curves represent the approximate results evaluated by $\delta\lambda_R=\delta n_0\times S$. In Fig.6, the lines represent $\delta\lambda_R=\delta n_0\times S_{n,o}$ and $\delta\lambda_R=\delta n_0\times S_{n,i}$. As shown in Fig. 6, the sensitivities for OM and IM are 38.29 nm/RIU and

10.082 nm/RIU, respectively. In this case, the sensitivity for the OM is larger than that for the IM. Hence, the resonant wavelength of the outer layer is more suitable to detect the RI change. Furthermore, the value of the sensitivity in this point (38.29 nm/RIU) is the largest in comparison with 34.43 nm/RIU for a single-layer-coated microsphere with a fixed radius R and the same layer thickness d=200 nm and just 8.23 nm/RIU for an uncoated microsphere with a fixed radius R=3.5 μm. Moreover, the performance of the coated WGMs based optical RI sensors is better than 30 nm/RIU for the fused silica microsphere (R=55 μm)[5]. These results imply that the triple-layer-coated microsphere can be attributed to improve the sensitivity of the coated microsphere structure. Our results should lead to the development of highly sensitive label-free sensors for bio-detection and chemical analysis.

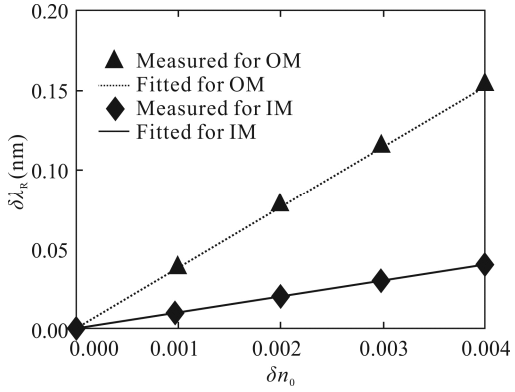

Fig.6 The sensitivities for OM and IM to detect the RI change of the surrounding medium

In summary, a micro-structure of triple-layer-coated microsphere resonator coupled with a phased matched waveguide is studied numerically using a 2D model based on the FDTD method. The relative intensity spectra, mode volume and EM field distribution are obtained. The WGMs in two high-RI layers can be efficiently excited by optimizing the coupling structure. The intrinsic mode of our microsphere presents two kinds of cladding modes (OM and IM), which makes it have more freedom degrees than the other microspheres. As for the RI sensing application, an increased sensitivity of 38.29 nm/RIU is achieved compared with the microsphere coated single-layer and the uncoated microsphere. The coating film can be achieved by the RF sputtering method, which allows various coating materials and controls the coating film easily. We believe that the results will expand the application of WGM resonator in sensing applications.

References

[1] Vahala K. J., Nature **424**, 839 (2003).
[2] Yang S., Wang Y. and Sun H., Advanced Optical Materials **3**, 1136 (2015).
[3] Dong Y., Wang K. and Jin X., Applied Optics **54**, 277 (2015).
[4] Bao J., Yu K., Wang L. and Yin J., Optoelectronics Letters **13**, 268 (2017).
[5] Li J., Xiao Y., Dong W. and Zhang X., Optoelectronics Letters **12**, 276 (2016).
[6] Righini G. C. and Soria S., Sensors **16**, 905 (2016).
[7] Foreman M. R., Swaim J. D. and Vollmer F., Advances in Optics and Photonics **7**, 168 (2015).
[8] Hanumegowda N. M., Stica C. J., Patel B. C., White I. M. and Fan X., Applied Physics Letters **87**, 201107 (2005).
[9] I. Teraoka and S. Arnold, Journal of the Optical Society of America B **24**, 653 (2007).
[10] Teraoka I. and Arnol, S., Optics Letters **32**, 1147 (2007).
[11] Hall J. M., Afshar V. S., Henderson M. R., Reynolds T., Riesen N. and Monro T. M., Optics Express **23**, 9924 (2015).
[12] Jin X., Wang J., Wang M., Dong Y., Li F. and Wang K., Applied Optics **56**, 8023 (2017).
[13] Wang M. Y., Jin X. Y.,Wang J., Chen L. M. and Wang K. Y., Acta Photonica Sinica **46**, 0706003 (2017). (in Chinese)
[14] Shen Z., Zhou Z. H., Zou C. L., Sun F. W., Guo G. P., Dong C. H. and Guo G. C., Photonics Research **3**, 243 (2015).
[15] Park J., Ozdemir S. K., Monifi F., Chadha T., Huang S. H., Biswas P. and Yang L., Advanced Optical Materials **2**, 711 (2014).
[16] Choy J. T., Bradley J. D., Deotare P. B., Burgess I. B., Evans C. C., Mazur E. and Lončar M., Optics Letters **37**, 539 (2012).